



UNIVERSITY OF

LIVERPOOL

Institute of Integrative Biology

Interactions of fibroblast growth factors with glycosaminoglycan brushes and the
pericellular matrix.

Thesis submitted in accordance with the requirements of the University of Liverpool
for the degree of doctor in Philosophy

BARADJI Aïseta

September 2017

ProQuest Number:28208881

All rights reserved

INFORMATION TO ALL USERS

The quality of this reproduction is dependent on the quality of the copy submitted.

In the unlikely event that the author did not send a complete manuscript and there are missing pages, these will be noted. Also, if material had to be removed, a note will indicate the deletion.



ProQuest 28208881

Published by ProQuest LLC (2020). Copyright of the Dissertation is held by the Author.

All Rights Reserved.

This work is protected against unauthorized copying under Title 17, United States Code
Microform Edition © ProQuest LLC.

ProQuest LLC
789 East Eisenhower Parkway
P.O. Box 1346
Ann Arbor, MI 48106 - 1346

Author's declaration

I declare that the work in this dissertation was carried out in accordance with the regulations of the University of Liverpool and the CIC BiomaGUNE. The study described is original and have not been submitted for any other degree. All aspects of the experimental design and planning for the study were conducted by me under the guidance and agreement of my supervisors, Professor David G. Fernig, Dr. Ralf P. Richter and Dr. Edwin Yates. The experimental work in this study was undertaken by me, with specific contributions that are indicated in the core of the thesis when appropriate.

Any views and hypothesis presented in this thesis are from the author and to not represent those of the University of Liverpool. This thesis has not been presented to any other university for examination in the United Kingdom or overseas.

PREVIEW

Acknowledgments

I would like to express my gratitude to the people who contributed by their support, guidance and advice to this study and my training.

This work would not have been possible without the input of many people but first and foremost, I would like to express my thankfulness to my supervisors, Professor **David G. Fernig**, Dr. **Ralf P. Richter** and Dr. **Edwin Yates** for their guidance and support throughout this four years of training in conducting research and personal development.

I am grateful to my assessors who guided me throughout this journey: Pr. **Olga Mayans**, Dr. **David Adams** and Dr. **Igor Baruskov**. Special thanks to Pr. **Jeremy Turnbull** and Pr. **Catherine Picart**, my internal and external examiners respectively for giving their final review to this work.

I would like to thank the people who I have worked along and who advised me in multiple occasions in the biosurfaces laboratory at the CIC BiomaGUNE and the biochemistry laboratory at the Institute of Integrative Biology: **Yong Li**, **Elisa Migliorini**, the group members and supporting staff of both laboratories. Thanks to Thao Bui, Pawin Ngamlert, Dunhao Sun and Zaid Alghair for their daily support and friendships.

Thanks to my friends and family for their continuous support on this journey. I could not possibly be thankful enough to my mother, **Dianessy Hawa**, for always being by my side and supporting my will of studying science.

“Success is not an end in itself. It is a journey that is best judged by the number of times that the traveller has been able to stand up after he/she has fallen down.”

H.E Ameenah Gurib-Fakim

PREVIEW

Abstract

The components of the extracellular matrix (ECM) are produced *in situ* by cells and are either completely secreted from the cell into the ECM or remain associated with the cell membrane. Amongst them are polysaccharides of the glycosaminoglycans (GAG) family, which are either free or covalently bound to proteins to make proteoglycans (PGs). These form a highly-hydrated compartment in which the proteins are embedded. At the molecular level, all ECM components are structured to execute their function and have been implicated in regulating intercellular communication. The sulfated GAGs interact with a wide range of proteins and their structure and tissue localisation is related to their function. Thus, certain GAGs may be particularly enriched in specific tissues, *e.g.*, dermatan sulfate in skin, but they are found in all tissues; and heparan sulfate (HS) has the widest range of interacting protein partners. These partners include both the permanent ECM residents and the transients, such as the fibroblast growth factors (FGFs), which transmit signals from one cell to another in paracrine signalling involved in tissue development, differentiation and homeostasis. The aims of this thesis are (1) to use a simple biomimetic model of ECM in the form of a GAG brush to determine if FGF binding leads to different supramolecular structures. (2) To determine if these supramolecular arrangements allow FGF mobility as observed *in vivo*. The model GAG brush was assembled layer by layer by one-end grafting of biotinylated GAGs on a streptavidin monolayer, itself attached to a supported lipid bilayer. The structure of these brushes was probed using different recombinant human FGFs (FGF1, HaloFGF1, FGF2, HaloFGF2, FGF4, HaloFGF6, FGF9, FGF10, HaloFGF10, FGF17, FGF18 and HaloFGF20) with well characterised HS binding sites (HBSs) and where “Halo” refers to an N-terminal Halotag fused to the FGF for fluorescence labelling. Rigidification of soft and highly hydrated films was assessed by quartz crystal microbalance with dissipation monitoring (QCM-D), spectroscopic ellipsometry (SE) was used to quantify the biomolecules at the surface, and fluorescence recovery after photobleaching (FRAP) was employed to assess the lateral diffusion of the GAGs and the (Halo)FGFs. FGFs showed a preference in binding stoichiometry for specific disaccharide structures, and the ensuing interactions led to different supramolecular

organisations of the brush/FGF films. Upon binding to the brushes, FGFs possessing multiple HBSs ('multivalent' FGFs) with acidic borders delimiting their HBSs were able to immobilise the GAG chains; some of these FGFs, *e.g.* HaloFGF1, remained mobile, whereas others were trapped in the film, *e.g.* HaloFGF2. Monovalent FGFs, and multivalent FGFs with no acidic borders around their HBSs, were found to not cross-link the brushes and remained mobile.

To test the idea that acidic borders on the protein surface play an important role in determining the ability of an FGF to cross-link HS chains and thus regulate mobility of the FGF in the matrix, the behaviour of fluorescently labelled Halo-FGFs were measured in the native pericellular matrix of fixed human keratinocytes. HaloFGF2 was immobile in HS brushes and in the pericellular matrix of HaCaT cells. This indicates that although the other components of the pericellular matrix may also play roles in determining the diffusion dynamics of FGF2, HS would be the main director of it.

Interactions between growth factors such as FGFs with components of the ECM are specific to their molecular features and can be precisely monitored in biomimetic models. These interactions trigger supramolecular structures that can be characterised by their stiffness. It is also possible to assess the mobility of these growth factors using a fluorescent label. Interestingly, the mobility of at least HaloFGF1, HaloFGF2 and HaloFGF10 in HS brushes was reproduced in pericellular matrix of HaCaT cells. A key difference is that the local supramolecular arrangement of the pericellular matrix components will be heavily influenced by the interactions of the HS chains with endogenous HS binding proteins. This will form a network of binding sites for FGFs, which at least in the case of HaloFGF2, did not prevent the immobilisation of the growth factor. However, in the case of other FGFs, *e.g.* HaloFGF6 and HaloFGF20 we detected reduced mobility. Thus, bridging the gap between the analyses on the HS brush model and on pericellular matrix may require the elaboration of a more complex *in vitro* model, incorporating other molecules into the HS brush, such as collagens and fibronectin, which have multiple HBSs and would be expected to present to the FGF already cross-linked HS chains and a reduced number of available binding sites.

Content

Author's declaration	i
Acknowledgments.....	ii
Abstract.....	iv
Content.....	vi
List of figures.....	x
List of tables	xiii
List of supplementary figures.....	xiv
List of abbreviations.....	xvii
1 Introduction	1
1.1 Cell communication in multicellular organisms.....	1
1.2 Extracellular matrix	2
1.3 The glycosaminoglycans of the ECM.....	4
1.3.1 Heparan sulfate and heparin	4
1.3.2 Chondroitin sulfate and dermatan sulfate.....	7
1.3.3 Molecular features, conformation and protein binding.....	8
1.4 Fibroblast growth factors: structures, functions and interactions with the ECM. 9	
1.4.1 Historical discovery	10
1.4.2 Structure-function relationship in FGFs and consequences for HS binding.	13
1.5 FGF and polysaccharide interactions.	18
1.6 Other methods for studying FGF and GAG interactions.....	19
1.6.1 Quartz crystal microbalance with dissipation monitoring (QCM-D).	19
1.6.2 Spectroscopic ellipsometry.....	21
1.6.3 Confocal microscopy.....	24

2	Aims and objectives	26
3	Experimental strategy.....	27
3.1	A well-defined biomimetic model of the ECM.....	27
3.2	Production and purification of FGF proteins	28
3.3	Quartz crystal microbalance with dissipation monitoring and spectroscopic ellipsometry monitoring of the establishment of ECM models.....	28
3.4	FRAP assessment of FGF interaction with HS films.	29
4	Methods.....	30
4.1	FGF production, purification and molecular biology	30
4.1.1	Media, buffers and plate preparation	30
4.1.2	Expansion of competent cells (DH5 α and C41 (DE3) pLysS).....	30
4.1.3	Plasmid design, transformation and amplification	31
4.1.4	Protein expression and purification.....	32
4.1.5	SDS-PAGE electrophoresis	34
4.2	Supported extracellular matrix models.	35
4.2.1	Treatment of substrates for QCM-D, SE and FRAP measurements.....	35
4.2.2	Preparation of small unilamellar vesicles (SUV) for supported lipid bilayers.....	36
4.2.3	Biotinylated glycosaminoglycans	37
4.3	Quartz crystal microbalance with dissipation monitoring (QCM-D).	38
4.4	Quartz crystal microbalance with dissipation monitoring (QCM-D).	38
4.5	Spectroscopic ellipsometry applied to ECM models.....	39
4.6	FRAP of extracellular matrix models.....	40
4.6.1	FRAP assessment of the lateral mobility of GAG	41
4.6.2	FRAP assessment of growth factor mobility	42
4.6.3	FRAP of labelled FGFs on HaCaT cells	44

4.6.4	Fluorescence recovery curves.....	45
4.7	Preparation of native extracellular matrix from eukaryotic cells.....	47
4.7.1	Cell culture routine	47
4.7.2	Fixation of HaCaT cells	48
5	Surface charges and heparin binding site distribution regulate dynamics of fibroblast growth factors in extracellular matrix models.....	49
5.1	Introduction	49
5.2	Manuscript	51
5.3	A HBS3- mutant of FGF2 also rigidifies and immobilizes HS brushes	99
5.4	Discussion.....	104
6	Interaction of FGFs with brushes formed with different GAGs.....	106
6.1	Introduction	106
6.1.1	Origin, composition and structural characteristics of GAGs.....	106
6.1.2	Characterization of GAG brushes.....	107
6.2	Interaction of members of the FGF1 subfamily with sulfated GAGs.....	109
6.2.1	Binding of FGF1 and FGF2 to GAG brushes.....	110
6.2.2	Rigidification of GAG brushes by members of the FGF1 subfamily.....	112
6.2.3	Binding stoichiometries of the FGF1 subfamily.	114
6.2.4	Cross-linking of GAG brushes by FGF1 and FGF2.....	115
6.3	Interactions of FGF4, FGF9, FGF10, FGF17 and FGF18 with GAG brushes. 117	
6.3.1	Binding of FGFs to GAG brushes	118
6.3.2	Rigidification of GAG brushes by FGFs.....	118
6.3.3	Stoichiometries of FGF binding to GAGs.....	121
6.4	Discussion.....	123
	Supplementary information.....	125

7	Mobility of FGFs in pericellular matrices	135
7.1	Introduction	135
7.2	HaloFGFs bind to the pericellular matrix of keratinocytes.....	135
7.2.1	Binding propensity and repartition.....	135
7.2.2	HaloFGF mobility in native pericellular matrices	139
7.3	Comparison of FGF mobility in HS brushes and pericellular matrices.....	142
7.4	Discussion.....	144
	Supplementary figures	145
8	Discussion and further work.....	149
8.1	General discussion	149
8.2	Further work	153
9	References	155

PREVIEW

List of figures

Figure 1.1: Forms of signalling in cellular communication.	2
Figure 1.2: Schematic representation of the extracellular matrix proteoglycan organisation.	3
Figure 1.3: Heparan sulfate disaccharide repeat unit.....	6
Figure 1.4: Model of alternating sulfation domains in HS proteoglycans.	7
Figure 1.5: Chondroitin sulfate disaccharide repeat unit.	8
Figure 1.6: Conformational changes in saccharide rings.	9
Figure 1.7: Radial phylogram of the FGF family.....	13
Figure 1.8: β -trefoil structure of FGFs.....	15
Figure 1.9: Surface electrostatic potential mapping and position of heparin binding lysines in FGF2.....	15
Figure 1.10: HBSs, sulfation pattern and oligosaccharide size preferences in FGF. ...	17
Figure 1.11: The working principle of QCM-D.	20
Figure 1.12: Polarization of light as an electromagnetic wave.....	21
Figure 1.13: Reflection of polarized light.....	23
Figure 1.14: Diagram of the confocal microscopy working principle.	25
Figure 3.1: HS brush – a well-defined ECM model.....	27
Figure 4.1: Schematic illustration of the custom-made sample holder for FRAP measurements.	41
Figure 4.2: Time resolved formation of streptavidin crystals for GAG immobilisation on a supported lipid bilayer.	44
Figure 4.3: Lateral mobility of an HS brush.....	46
Figure 4.4: Fluorescence recovery curve of HS brushes.	47
Figure 5.1: Phylogenetic tree of FGFs.	49
Figure 5.2: Representative sketch of HS brushes as a well-defined ECM model.	62
Figure 5.3: QCM-D monitoring of the formation of a mid-dense (A) and a dense (B) HS brush.	62
Figure 5.4: QCM-D monitoring of FGFs from the FGF1 subfamily binding to a mid-dense HS brush.....	65
Figure 5.5: FGFs from the FGF1 subfamily bind and rigidify HS brushes.....	66

Figure 5.6: Stoichiometry of FGF binding to HS, for proteins of the FGF1 subfamily	67
Figure 5.7: FGF2 reduces HS mobility but FGF1 does not.	68
Figure 5.8: QCM-D monitoring of FGF binding to HS brushes.	71
Figure 5.9: HS film rigidification by FGFs from subfamilies other than FGF1	72
Figure 5.10: Stoichiometry of FGF binding to HS, for all tested FGFs. The molar FGF surface densities were determined by SE at equilibrium after incubation at 0.28 μ M, and after rinsing with working buffer for a minimum of 60 minutes, and compared to molar HS surface densities obtained in the same measurements. The data presented is for two independent measurements, and the mean values and standard deviations are indicated.	73
Figure 5.11: Mobility of FGF bound HS brushes as observed in FRAP.....	75
Figure 5.12: Mid-dense HS film rigidification by HaloFGFs.....	77
Figure 5.13: Quantification of HaloFGF binding to mid-dense and dense HS brushes.	78
Figure 5.14: Mobility of HaloFGFs in HS films.....	80
Figure 5.15: Surface electrostatic potential mapping and position of heparin binding lysines in FGF2.....	81
Figure 5.16: Surface electrostatic potential mapping and position of heparin binding lysines in FGF1.....	81
Figure 5.17: Representative sketch of supramolecular events in HS-FGF brushes. ...	82
Figure 5.18: QCM-D monitoring of FGF2 HBS3- binding to a mid-dense HS brush.	100
Figure 5.19: Stoichiometry of FGF2 and FGF2 HBS3- binding to HS.	101
Figure 5.20: HBS3 mutant of FGF2 subfamily bind and rigidify HS brushes.	101
Figure 5.21: FGF2 and FGF2 HBS3- immobilise HS with different potencies.....	103
Figure 5.22: Quantitative analysis of the effect of FGF2 and FGF2 HBS3- on HS mobility.	104
Figure 6.1: Characterisation of mid-dense GAG brushes.....	108
Figure 6.2: Comparative parametric plot analysis of the interaction of members of the FGF1 subfamily with GAG brushes.	112
Figure 6.3: Stoichiometry of binding of members of the FGF1 subfamily to GAG brushes.....	115
Figure 6.4: Mobility of GAG chains in GAG brushes with FGF1 or FGF2.....	117

Figure 6.5: Parametric plot analysis of FGFs interaction with GAG brushes.	120
Figure 6.6: Stoichiometric quantification of FGF bound to GAG brushes.	122
Figure 7.1: Non-specific binding control of TMR and TMR-Halotag on HaCaT cells.	136
Figure 7.2: Fluorescent labelling the pericellular matrix of HaCaT cells with HaloFGFs.	137
Figure 7.3: Average binding intensities of HaloFGFs to the pericellular matrix of HACaT.....	138
Figure 7.4: Fluorescence recovery of HaloFGFs following photobleaching in the pericellular matrix of HaCaT cells.....	141
Figure 7.5: Comparison of mobility of HaloFGFs in HS brushes and native pericellular matrices.....	143

PREVIEW

List of tables

Table 1: SDS PAGE gel preparation recipe	35
Table 2: Disaccharide repeat of glycosaminoglycans.	38

PREVIEW

List of supplementary figures

Supplementary figure 5.1: Quantitative characterisation of a mid-dense HS brush by SE.....	89
Supplementary figure 5.2: Quantitative analysis of the effect of FGF1 and FGF2 on HS mobility.	90
Supplementary figure 5.3: Surface electrostatic potential mapping and position of heparin binding lysines in FGF4.	91
Supplementary figure 5.4: Surface electrostatic potential mapping and position of heparin binding lysines in FGF9.	91
Supplementary figure 5.5: Quantitative analysis of the effect of FGFs on HS mobility.	92
Supplementary figure 5.6: Surface electrostatic potential mapping and position of heparin binding lysines in FGF10.	93
Supplementary figure 5.7: Surface electrostatic potential mapping and position of hepbinding lysines in FGF17.....	93
Supplementary figure 5.8: Surface electrostatic potential mapping and position of heparin binding lysines in FGF18.	94
Supplementary figure 5.9: SAV-coated SLBs are inert to FGF binding as monitored by QCM-D.....	95
Supplementary figure 5.10: QCM-D monitoring of HaloFGF binding to mid-dense HS films.....	96
Supplementary figure 5.11: Illustration of FRAP of biomolecules in the ECM models.	97
Supplementary figure 5.12: Quantitative analysis of HaloFGF mobility in HS films..	98
Supplementary figure 5.13: Quantitative analysis of the effect of HaloFGFs on HS mobility.	98
Supplementary figure 6.1: QCM-D monitoring of FGF1 interaction with mid-dense GAG brushes.....	125
Supplementary Figure 6.2: QCM-D monitoring of FGF2 interaction with mid-dense GAG brushes.....	126

Supplementary figure 6.3: QCM-D monitoring of FGF2 HBS3- interaction with mid-dense GAG brushes.....	126
Supplementary figure 6.4: Stoichiometry of binding of members of the FGF1 subfamily to GAG brushes.....	127
Supplementary Figure 6.5: Parametric plot analysis of FGF1 interaction with mid-dense GAG brushes.....	127
Supplementary figure 6.6: Parametric plot analysis of FGF2 interaction with mid-dense GAG brushes.....	128
Supplementary figure 6.7: Parametric plot analysis of FGF2 HBS3- interaction with mid-dense GAG brushes.....	128
Supplementary Figure 6.8: Fluorescence recovery curves of mid-dense GAG brushes.....	129
Supplementary Figure 6.9: Mobility parameters of bare GAG brushes, and GAG brushes with bound FGF1 and FGF2.....	129
Supplementary Figure 6.10: QCM-D monitoring of FGF4 interaction with GAG brushes.....	130
Supplementary figure 6.11: Parametric plot analysis of FGF4 interaction with GAG brushes.....	130
Supplementary figure 6.12: QCMD monitoring of FGF9 interaction with GAG.	131
Supplementary figure 6.13: Parametric plot analysis of FGF9 interaction with GAGs.....	131
Supplementary figure 6.14: QCMD monitoring of FGF10 interaction with GAG. ...	132
Supplementary figure 6.15: Parametric plot analysis of FGF10 interaction with GAGs.....	132
Supplementary figure 6.16: QCMD monitoring of FGF17 interaction with GAG. ...	133
Supplementary figure 6.17: Parametric plot analysis of FGF17 interaction with GAGs.....	133
Supplementary figure 6.18: QCMD monitoring of FGF18 interaction with GAG. ...	134
Supplementary figure 6.19: Parametric plot analysis of FGF18 interaction with GAGs.....	134
Supplementary figure 7.1: mean comparison of HaloFGF binding intensities.....	145

Supplementary figure 7.2: Mobility parameters of HaloFGFs in the pericellular matrix of HaCaT.....	146
Supplementary figure 7.3: FRAP images of HaloFGFs on HaCaT cells.	147
Supplementary figure 7.4: FRAP images of HaloFGFs on HaCaT cells.	148

PREVIEW

List of abbreviations

BSA: Bovine serum albumin

CS: Chondroitin sulfate

CS-A : Chondroitin sulfate A

CS-C : Chondroitin sulfate C

CS-D : Chondroitin sulfate D

CS-E: Chondroitin sulfate E

DMEM: Dulbecco's modified Eagle medium

DMSO: Dimethylsulfoxide

DOPC: 1, 2-Dioleoyl-*sn*-Glycero-3-phosphocholine

DOPE-CAP-B: 1, 2-Dioleoyl-*sn*-Glycero-3-phosphoethanolamine-cap-biotin

DTT: Dithiothreitol

dp: degree of polymerization

DS : Dermatan sulfate

ECM : Extracellular matrix

EXT: exotosin

EXTL: exotosin-like

FCS: foetal calf serum

FGF: Fibroblast growth factor

FGFR: fibroblast growth factor receptor

FRAP: Fluorescence recovery after photobleaching

GAGs: glycosaminoglycans

Gal: Galactose

GalNAc: N-acetylgalactosamine

GlcA: Glucuronic acid

GlcNAc: N-acetyl glucosamine

GlcNS: N-sulfated glucosamine

HA: Hyaluronic acid

HaloTag: haloalkane dehalogenase tag

Halo-FGF: FGF fused to an N-terminal HaloTag

HB: HEPES buffer: 150 mM NaCl, 10 mM HEPES, pH 7.4

HBS: Heparin binding site

Hep: Heparin

HS: Heparan sulfate

HSPG: Heparan sulfate proteoglycans

IdoA: Iduronic acid

IPTG: isopropyl β -D-1-thiogalactopyranoside

LB: Lysogeny broth

MMPs: matrix metalloproteases

NDST: N-deacetylase/N-sulfotransferase

OD600: optical density at 600 nm

ON: overnight

OST: O-sulfotransferase

PAGE: polyacrylamide gel electrophoresis

PBS: phosphate-buffered saline

PDB: Protein data bank

PFA: paraformaldehyde

PGs: Proteoglycans

QCM-D: Quartz crystal microbalance with dissipation

ROI: region of interest

RT: room temperature

SAv: Streptavidin

SDS: Sodium dodecylsulfate

SE: Spectroscopic ellipsometry

SLB: Supported lipid bilayer

SUV: Small unilamellar vesicles

SPDBV: Swiss PDB viewer

TEMED: N, N, N', N'-Tetramethylethylenediamine

Tris: Tris (hydroxymethyl) methylamine

TPA: Time-resolved profile analysis

UDP: Uracil diphosphate

Xyl: Xylose

PREVIEW

1 Introduction

1.1 Cell communication in multicellular organisms.

In multicellular organisms, intercellular communication processes are the foundation of their growth and expansion, development, function, integrity and regeneration. Intercellular communication happens via various modes, the cell can target itself, a process that is called “autocrine” signalling or a neighbouring cell by direct molecular contacts (juxtacrine signalling) or cytoplasm contacts through gap junctions (1). Paracrine signalling is the local communication between cells without a direct molecular physical contact. Chemokines, cytokines, growth factors and many morphogens are paracrine signalling agents. They are secreted into the pericellular matrix of the source cell, and travel throughout the interstitial matrix towards the target cells. On the target cell, the paracrine effector binds to a receptor that triggers downstream signalling within the cell (2). This is the case of fibroblast growth factors (FGFs) signalling via tyrosine kinase receptors (3) and transforming growth factors family members such as the bone morphogenetic proteins that bind to the bone morphogenetic protein receptor type II in development processes (4). Intercellular communication can happen over longer distances, in which case the secreted effector travels through the endothelial barrier and is transported in the vascular blood flow throughout the body, but only acts on cells expressing the cognate receptor. This is the endocrine system and concerns hormones (Figure 1.1). The extracellular matrix (ECM) is the extracellular environment in contact with the cell; it is implicated in controlling cell fate decisions. During development, morphogen gradients are shaped by ECM components, whereas in homeostasis the ECM takes part in tissue regeneration and immunity by controlling the activity and transport of proteins regulating cell growth, migration and differentiation. Besides the components, the physical characteristics of the ECM are also relevant. It was shown that the elasticity of the ECM controls the differentiation of stem cells (5) and the polarisation of fibroblasts has been related to the stiffness of ECM (6). Stiffness and elasticity are both determined by the supramolecular structure of ECM, which in turn

depends on its molecular composition and the interactions of the component molecules.

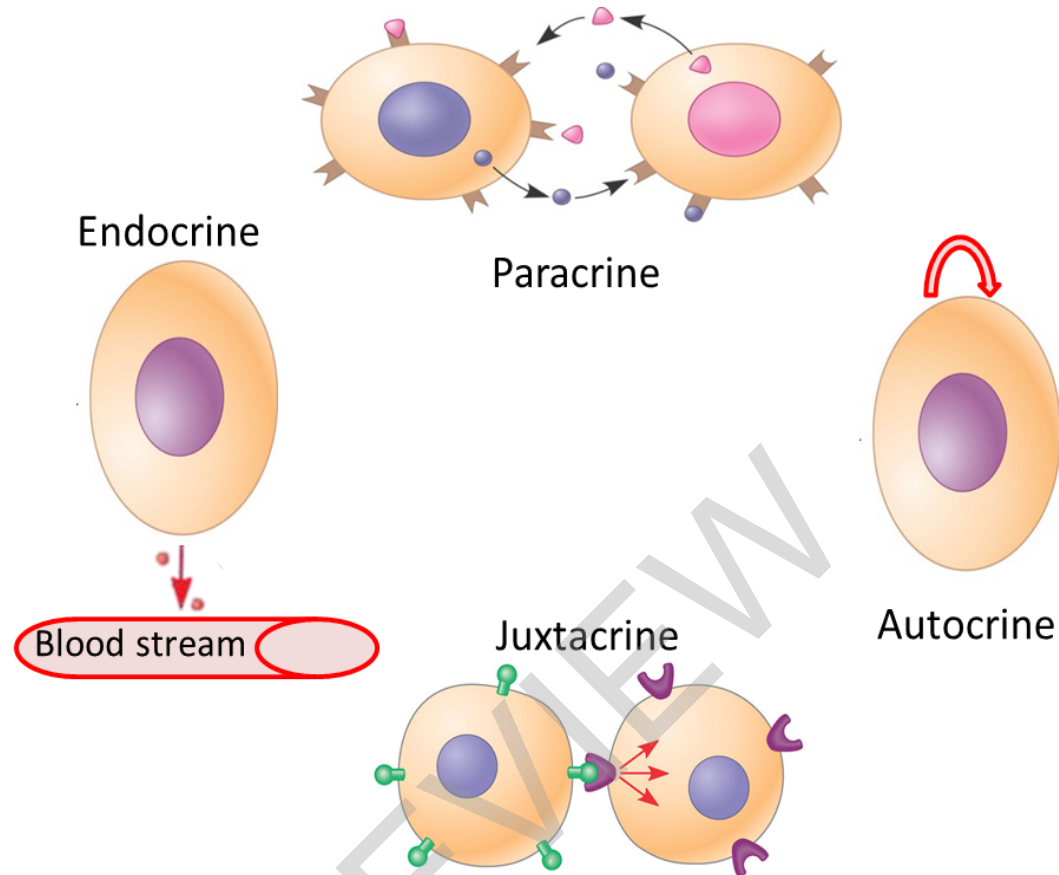


Figure 1.1: Forms of signalling in cellular communication.

Endocrine signalling corresponds to the intercellular communication that occurs via transport of the effector by the blood stream. Juxtacrine communication involves contact between the signalling and the targeted cell as described in the figure. Autocrine signalling depicts the signalling of a cell on itself and the paracrine signalling the one to a neighbouring cell. In paracrine and autocrine signalling, the effector molecule is transported in the immediate microenvironment of the cells that is the extracellular matrix.

1.2 Extracellular matrix

The ECM has distinct domains, the pericellular matrix is immediately adjacent to the cell surface, extending 1-5 μm in some tissues (7). Further away in mesenchymal tissues is the interstitial matrix. In epithelial tissues and the vasculature, a specialised ECM is found beyond the pericellular matrix, the basement membrane, so called due to its molecular density causing it to be heavily stained in a number of classic histological preparations. Basement membrane separates these compartments from

the underlying mesenchyme (8) (Figure 1.2). At the molecular level, all ECM have reasonably well-studied components and these are mainly fibrous proteins such as collagens, and the polysaccharides of the glycosaminoglycan (GAGs) family.

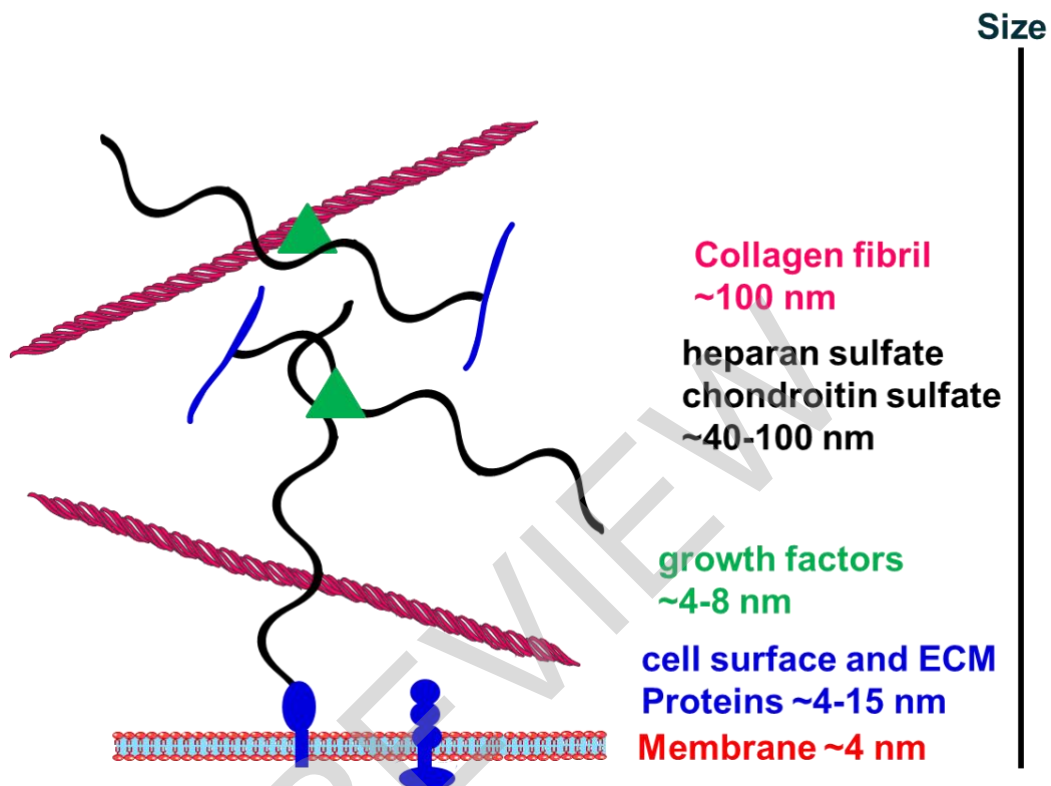


Figure 1.2: Schematic representation of the extracellular matrix proteoglycan organisation. Here schematized are the ECM with collagen fibrils and GAGs. HSPGs core proteins (blue) carrying HS chains (black) are sitting in the ECM or anchored in the cell membrane, with bound growth factor (green).

Collagens are the scaffold of extracellular matrices. They are tissue specific, organised in fibrils and provide resistance to shear and pressure (9). Type I and type III collagens sit in the interstitial matrices of soft tissues, *e.g.*, the dermis (10). In bones, collagen I fibrils can represent up to 90% of matrix protein components (11). Collagen type IV is the fibrous components of the basement membranes and is connected to the interstitial matrix via collagen VI, thus the fibrous scaffolds of basement membrane and the interstitial matrix form interconnected networks (12). Along with collagen type IV, fibronectins, laminins, nidogen and perlecan are the main constituents of the basement membrane. Laminins are connected to collagen IV and perlecans by nidogens (13). The ECM is a complex network where the main